

Single-phase flow simulation in 3-D naturally fractured reservoirs using a locally conservative formulation, an embedded discrete fracture model and unstructured tetrahedral meshes

Túlio de M. Cavalcante¹, Darlan K. E. Carvalho², Paulo R. M. Lyra²

¹*Dept. of Civil Engineering, Federal University of Pernambuco
Av. Arquitetura s/n, Cidade Universitária, Recife, CEP 50740-550, PE, Brazil.
tulio.cavalcante@ufpe.br*

²*Dept. of Mechanical Engineering, Federal University of Pernambuco
Av. Arquitetura s/n, Cidade Universitária, Recife, CEP 50740-550, PE, Brazil.
darlan.ecarvalho@ufpe.br, paulo.lyra@ufpe.br*

Abstract. Fluid flow in fractured porous media is a truly relevant phenomenon for the oil industry, but also for water extraction and aquifer remediation. Modeling this type of problem represents a great challenge, due to the complexity of depositional environments. In such cases, it is particularly complex to construct structured meshes capable of adequately modeling the reservoir. In this context, in the present paper, we describe a new strategy to simulate the single-phase fluid flows in three-dimensional heterogeneous, anisotropic and fractured porous media using tetrahedral unstructured meshes. Aiming to model fractures, we use the Embedded Discrete Fracture Model (EDFM) in which fractures are represented explicitly, but without the necessity of building a “fracture fitting mesh”, which could be an overly complex task. To discretize the elliptic pressure equation, we use the recently developed 3-D version of the MultiPoint Flux Approximation that uses the "Diamond stencil" (MPFA-D) which is a robust and flexible formulation, capable of handling highly heterogeneous and anisotropic reservoir rocks, achieving second order accuracy for the scalar variable and first order accuracy for fluxes. Our strategy has shown to be notably flexible, and our preliminary results are very promising.

has achieved good preliminary results.

Keywords: naturally fractured reservoirs, single-phase flow, embedded discrete fracture model (EDFM), multipoint flux approximation with a diamond scheme (MPFA-D), tetrahedral meshes.

1 Introduction

Fluid flow in fractured porous media is a relevant phenomenon, not only because most of the remaining oil reserves around the world reside in fractured reservoirs [1], but also due to the fact that fractures are also present in less deep layers of the crust, which makes them also important in water extraction and aquifer remediation [2]. The objective of this work is to numerically simulate the single-phase flow in 3-D naturally fractured reservoirs. Modeling this problem is a great challenge, due to the complexity of depositional environments, in which some properties as permeability, for example, may vary many orders of magnitude over small distances, in addition to the presence of the fractures [3]. These environments are, moreover, anisotropic media, since the sedimentary layers can be deposited in different ways, giving different preferential directions to the fluids flows [3], what makes particularly complex, in such cases, to construct structured k-orthogonal meshes capable of modeling this type of media adequacy [4]. In this context, the presence of the fractures, which potentially introduce discontinuities on the pressure or the velocity fields [5], represents an additional difficulty, since their influence on the fluid flow must be correctly included in the model.

The models that represent fractures explicitly, treating them as additional degrees of freedom, may achieve

more accurate and physics-based results than traditional methods [6], as transmissibility multipliers [7] or dual-porosity models [8]. Explicit fracture representation methods can be divided into two groups, based on the way of the discretization: conforming mesh and non-conforming mesh methods. For the first group, the mesh needs to accommodate the fracture positions, which are placed at the cell edges (in 2-D) or faces (in 3-D). This condition is critical when it is necessary to discretize small angles and small distances and can lead to excessive refinements. This is not necessary for the second one, in which the fractures may cross the rock matrix mesh cells. The second group is less restrictive in terms of mesh construction, and we have decided to use it. In this context, we have used, to handle the fractures in this work, the embedded discrete fracture models (EDFM) [9], in which the degrees of freedom of the rock matrix and fractures are discretized separately, but the coupling terms are modeled in terms of discrete variables directly [10]. Referring to the numerical formulation to discretize the mathematical model (i.e., the elliptic pressure equation), we used the tridimensional extension of the multipoint flux approximation approach that uses the "diamond stencil" (MPFA-D) [11] with explicit weighting for the vertex unknowns. This method shows second-order accuracy for the scalar variable and first order accuracy for fluxes on arbitrary tetrahedral meshes. We have tested our strategy against some problems found in literature and our strategy has shown to be notably flexible with very good results for the evaluated problems.

2 Mathematical Formulation

The steady-state diffusion problem in 3-D can be described by [11]:

$$\vec{\nabla} \cdot \vec{\mathcal{F}} = \mathcal{Q}(\vec{x}), \quad \text{with } \vec{\mathcal{F}} = -\mathbf{K}(\vec{x})\nabla u \quad \text{in } \vec{x} = (x, y, z) \in \Omega \subset \mathbb{R}^3 \quad (1)$$

in which $\vec{\mathcal{F}}$ represents the diffusive flux, u is the scalar or potential variable, $\mathcal{Q}(\vec{x})$ is the source term and $\mathbf{K}(\vec{x})$ is the diffusion tensor that satisfies the ellipticity condition [12] and that can be written, in Cartesian coordinates, as:

$$\mathbf{K}(\vec{x}) = \begin{bmatrix} \kappa_{xx} & \kappa_{xy} & \kappa_{xz} \\ \kappa_{yx} & \kappa_{yy} & \kappa_{yz} \\ \kappa_{zx} & \kappa_{zy} & \kappa_{zz} \end{bmatrix} \quad (2)$$

Moreover, the appropriate boundary conditions are defined by:

$$\begin{cases} u = g_D & \text{on } \Gamma_D \\ \vec{\mathcal{F}} \cdot \vec{n} = g_N & \text{on } \Gamma_N \end{cases} \quad (3)$$

where the scalar functions g_D (prescribed values for u) and g_N (prescribed fluxes) are, respectively, defined on Γ_D (Dirichlet) and Γ_N (Neumann) boundaries, with $\partial\Omega = \Gamma_D \cup \Gamma_N$ and $\Gamma_D \cap \Gamma_N = \emptyset$, and \vec{n} is the unitary outward normal vector.

3 Numerical Formulation

In this section, we present the development of the EDFM for tetrahedral meshes and of the MPFA-D. Given a computational domain Ω with boundary Γ , we discretize it by a set of non-overlapping polyhedral control-volumes. Then, by integrating Eq. (1) and applying the Gauss's Divergence Theorem over the control-volume \hat{L} (with boundary $\Gamma_{\hat{L}}$ and volume $\Omega_{\hat{L}}$), we have:

$$\int_{\Gamma_{\hat{L}}} \vec{\mathcal{F}} \cdot \vec{n} \, d\Gamma_{\hat{L}} = \int_{\Omega_{\hat{L}}} \mathcal{Q} \, d\Omega_{\hat{L}} \quad (4)$$

By using the mean value theorem, we can write:

$$\sum_{\bar{f} \in \Gamma_{\hat{L}}} \vec{\mathcal{F}} \cdot \vec{N}|_{\bar{f}} = \bar{Q}_{\hat{L}} \Omega_{\hat{L}} \quad (5)$$

where $\bar{Q}_{\hat{L}}$ is the mean source term in \hat{L} and \bar{f} is a face belonging to $\Gamma_{\hat{L}}$, which is the set of boundary faces of the control-volume \hat{L} . In Eq. (5) different approximations for the flux expression $\vec{\mathcal{F}} \cdot \vec{N}$ produce different finite volume approximations.

3.1 The Multipoint Flux Approximation using the Diamond Stencil in 3-D

We start from the formulation presented by Lira Filho et al. [11], which is applicable to diffusion problems in 3-D tetrahedral meshes, in which the unique flux expression through a face, considering the configuration shown in Figure 1, is given by:

$$\vec{F} \cdot \vec{N} = -\mathfrak{K}|\vec{N}| \left[(u_R - u_L) - \frac{1}{2} \mathfrak{D}_{JK}(u_J - u_I) + \frac{1}{2} \mathfrak{D}_{JI}(u_J - u_K) \right] \quad (6)$$

with:

$$\mathfrak{K} = \frac{K_R^n K_L^n}{h_L K_R^n + h_R K_L^n} \quad (7)$$

$$\mathfrak{D}_{ij} = \frac{\langle \vec{\tau}_{ij}, \vec{L}\hat{R} \rangle}{|\vec{N}|^2} - \frac{1}{|\vec{N}|} \left(h_L \frac{K_L^{t,ij}}{K_L^n} + h_R \frac{K_R^{t,ij}}{K_R^n} \right); \quad i, j = I, J, K \quad (8)$$

where:

$$\vec{\tau}_{ij} = \vec{N} \times \vec{\alpha}_{ij}; \quad K_{\hat{\ell}}^n = \frac{\vec{N}^T \mathbf{K}_{\hat{\ell}} \vec{N}}{|\vec{N}|^2}; \quad K_{\hat{\ell}}^{t,ij} = \frac{\vec{N}^T \mathbf{K}_{\hat{\ell}} \vec{\tau}_{ij}}{|\vec{N}|^2}; \quad \hat{\ell} = L, R; \quad i, j = I, J, K \quad (9)$$

where $h_{\hat{\ell}}$ is the height from $\hat{\ell}$ ($\hat{\ell} = L, R$) to the face IJK , whose normal area vector is \vec{N} . In this formulation, the auxiliary vertex unknowns (u_I, u_J, u_K) could be interpolated as a weighting of the values of u at the cells sharing the respective node (I, J or K). We use the linearity-preserving interpolation strategy presented by Lira Filho et al. [11].

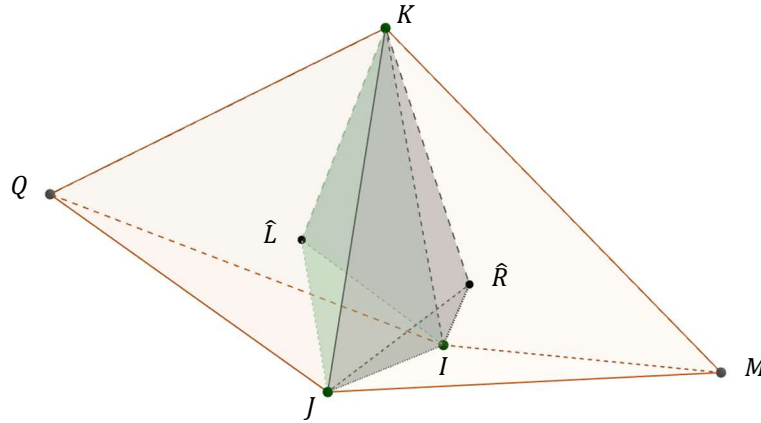


Figure 1 – Face IJK shared by the tetrahedrons \hat{L} and \hat{R} , highlighting \hat{L} and \hat{R} .

3.2 Fracture-Matrix and Fracture-Fracture Intersections Calculation

Let \hat{t} be a generic tetrahedron defined by the intersections of the planes π_1, π_2, π_3 and π_4 (with normal vectors $\vec{n}_1, \vec{n}_2, \vec{n}_3$ and \vec{n}_4) and let π_f be the plane containing the fracture f (with normal vector \vec{n}_f). Considering that \vec{P}_f is a point on π_f and that $\vec{T}_1, \vec{T}_2, \vec{T}_3$ and \vec{T}_4 are the vertices of \hat{t} , we can determine if there exist any intersection between \hat{t} and π_f , verifying if all the vertices of \hat{t} are in the same hemisphere, considering the two hemispaces defined by π_f . If it is false, then the intersection between \hat{t} and π_f exists. If $\pi_f \cap \hat{t} \neq \emptyset$, we can calculate the area of the intersection between the plane fracture and the tetrahedron through the following algorithm: Considering that \vec{P}_i is a point on π_i (as well as \vec{P}_f on π_f), the intersection between the planes defining \hat{t} two-by-two and the plane containing f will give rise to six linear systems as:

$$\begin{bmatrix} n_{ix} & n_{iy} & n_{iz} \\ n_{jx} & n_{jy} & n_{jz} \\ n_{fx} & n_{fy} & n_{fz} \end{bmatrix} \begin{bmatrix} x \\ y \\ z \end{bmatrix} = \begin{bmatrix} n_{ix}P_{ix} + n_{iy}P_{iy} + n_{iz}P_{iz} \\ n_{jx}P_{jx} + n_{jy}P_{jy} + n_{jz}P_{jz} \\ n_{fx}P_{fx} + n_{fy}P_{fy} + n_{fz}P_{fz} \end{bmatrix}; \quad \begin{matrix} i, j = 1, 2, 3, 4 \\ i \neq j \end{matrix} \quad (10)$$

whose solutions will define six points coordinates of which, however, only three or four will be on the faces of \hat{t} .

These three or four points will form the polygon $p = \pi_f \cap \hat{t}$, as shown in Figure 2.

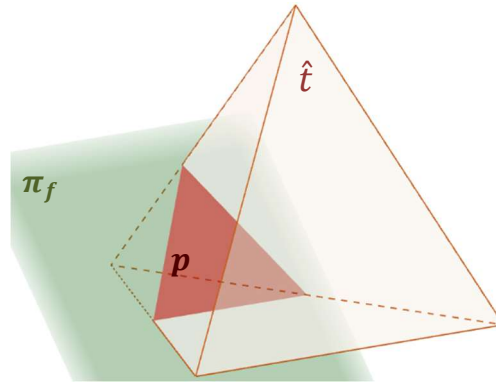


Figure 2 – Intersection between π and \hat{t} .

Thus, we have two coplanar polygons (f and p) intersecting each other, so that $q = f \cap p = f \cap \hat{t}$, as shown in Figure 3. Mathematically, it is obtained by the intersections between the straight lines containing the edges of f and p . Naturally, if f have n edges and p have m edges, we will obtain $n \cdot m$ intersection points, of which not all will be part of $q = f \cap p$, but only those within the limits of the edges of the polygons, together with the vertices of f inside p and the vertices of p inside f .

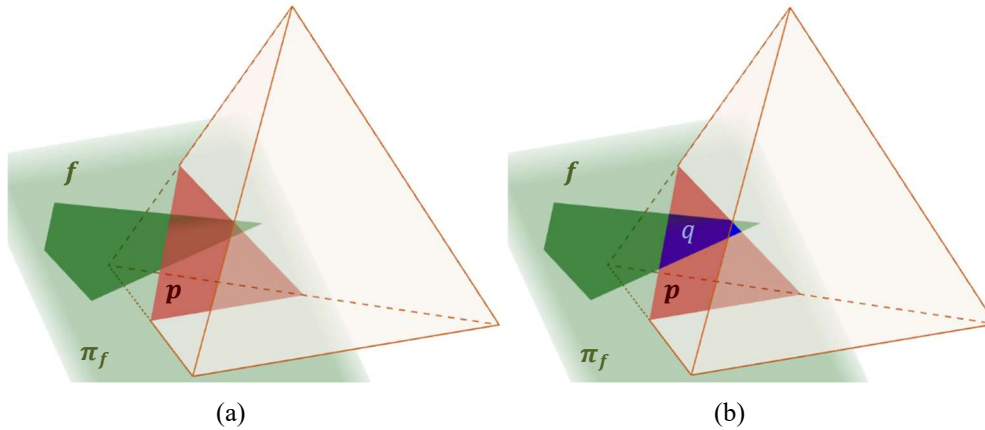


Figure 3 – Intersection between f and p . (a) f, p, \hat{t} . (b) $q = f \cap p = f \cap \hat{t}$.

The intersection between two plane fractures, whenever it is not parallel, in its turn, is made by the following algorithm: let π_{f_1} be the plane containing the fracture f_1 and let π_{f_2} be the plane containing the fracture f_2 . Let $r = \pi_{f_1} \cap \pi_{f_2}$ be a straight line coplanar to f_1 and to f_2 , this way we can determine the segments $s_1 = r \cap f_1$ and $s_2 = r \cap f_2$ (intersecting r with the straight lines containing the edges of f_1 and f_2), so that $f_1 \cap f_2 = s_1 \cap s_2$, as shown in Figure 4.

3.3 Fracture-Matrix and Fracture-Fracture Transmissibilities Calculation

The matrix-fracture transmissibility is calculated as [13]:

$$T_{\hat{t}f} = (T_{\hat{t}}^{-1} + T_f^{-1})^{-1} \quad (11)$$

where:

$$T_{\hat{t}} = \frac{2(\vec{n}^T \mathbf{K}_{\hat{t}} \vec{n}) A_{\hat{t}f}}{\langle d \rangle}; \quad T_f = \frac{2(\vec{n}^T \mathbf{K}_f \vec{n}) A_{\hat{t}f}}{w_f} \quad (12)$$

in which $A_{\hat{t}f}$ is the area of the intersection $f \cap \hat{t}$ (f is a fracture cell and \hat{t} is a rock matrix cell), \vec{n} is the unitary normal vector of the plane containing f . $\mathbf{K}_{\hat{t}}$ and \mathbf{K}_f are the permeabilities of \hat{t} and f , respectively, w_f is the aperture of the fracture f and:

$$\langle d \rangle = \frac{1}{\Omega_{\hat{t}}} \int_{\Omega_{\hat{t}}} |\vec{n} \cdot \vec{r}| \partial \Omega_{\hat{t}} \quad (13)$$

where \vec{r} is a vector from the center of $f \cap \hat{t}$ to a point in \hat{t} .

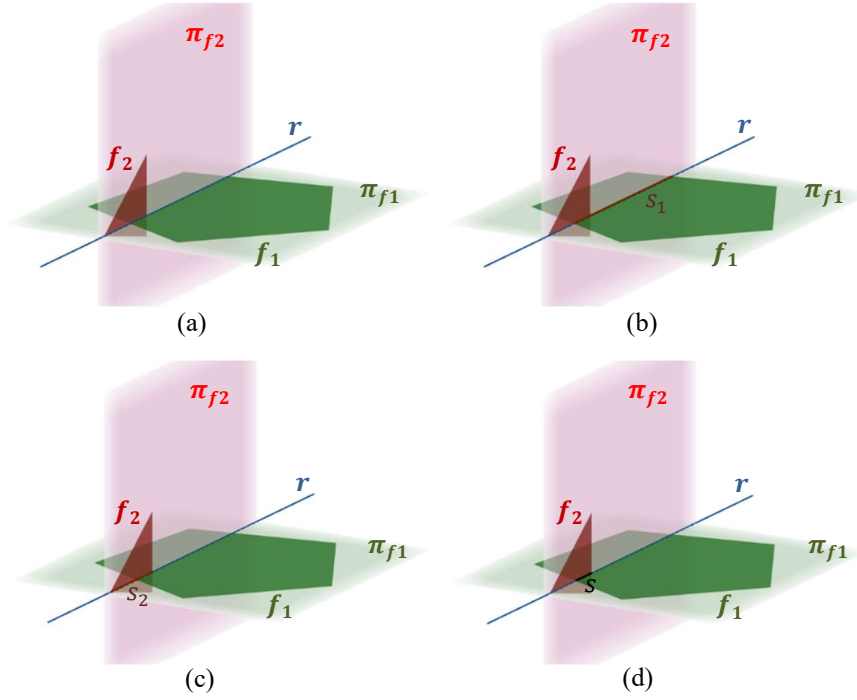


Figure 4 – Intersection between f_1 and f_2 . (a) $r = \pi_{f_1} \cap \pi_{f_2}$. (b) $s_1 = r \cap f_1$. (c) $s_2 = r \cap f_2$. (d) $s = s_1 \cap s_2 = f_1 \cap f_2$.

The fracture-fracture transmissibility is calculated as:

$$T_{f_1 f_2} = (T_{f_1}^{-1} + T_{f_2}^{-1})^{-1} \quad (14)$$

where:

$$T_{f_1} = \frac{2(\vec{n}_1^T \mathbf{K}_{f_1} \vec{n}_1) w_{f_1} L_{f_1 f_2}}{\langle d_{12} \rangle}; \quad T_{f_2} = \frac{2(\vec{n}_2^T \mathbf{K}_{f_2} \vec{n}_2) w_{f_2} L_{f_1 f_2}}{\langle d_{21} \rangle} \quad (15)$$

in which $L_{f_1 f_2}$ is the length of the intersection $f_1 \cap f_2$ (f_1 and f_2 are fracture cells), \vec{n}_i is the unitary normal vector of the plane containing f_i . \mathbf{K}_{f_i} is the permeability of f_i , w_{f_i} is the aperture of the fracture f_i ($i = 1, 2$) and:

$$\langle d_{ij} \rangle = \frac{1}{\Gamma_{f_i}} \int_{\Gamma_{f_i}} |\vec{n}_j \cdot \vec{s}| \partial \Gamma_{f_i} \quad (16)$$

where \vec{s} is a vector from the center of $f_1 \cap f_2$ to a point in f_1 .

4 Results

Here, we present the results for a 2-D one-phase flow problem and for its 3-D cubic extruded version: consider the one-phase flow in a 2-D domain defined as $\Omega = [0, 100]^2 \text{m}$, with prescribed pressure $p_i = 1$ bar at $\vec{x}_i = (0, 0)$ and prescribed flow $q_p = 10^{-5} \text{ m}^3/\text{d}$ at $\vec{x}_p = (100, 100)$, with isotropic permeability tensors for the rock matrix (m) and for the fracture (f) defined (in Darcy) as:

$$K_m = \begin{bmatrix} 10^{-5} & 0 \\ 0 & 10^{-5} \end{bmatrix}; K_f = \begin{bmatrix} 10^8 & 0 \\ 0 & 10^8 \end{bmatrix}; \quad (17)$$

The fractures are placed as shown in Figure 5a, in which we can also see the 2-D mesh (with 1,860 triangles). Through the strategy presented by Cavalcante et al. [14], which is a conforming mesh hybrid-grid method, we can obtain the solution for this problem, as shown Figure 5d, in which the calculated pressure at the production well is $p_p = 0.4750$ bar. This result was used as reference for comparison purposes. We have also solved a 3-D cubic extruded version of this problem, creating an unstructured mesh with 34,963 tetrahedral cells and including the contributions of the fractures as explained in this paper. The fractures were considered as two rectangles, each one corresponding to one “beam” of the cross, as shown in Figure 5b. We discretized the fractures by two ways: in the first one, we consider each rectangle as one additional degree of freedom, as shown in Figure 5b; in the second one, we divided each rectangle as eight triangles and each triangle is one additional degree of freedom, as shown in Figure 5c. The result of this 3-D problem is shown in Figure 5e (for the fractures discretization shown in Figure 5b) and in Figure 5f (for the fractures discretization shown in Figure 5c). In both cases, the calculated pressure at the production well is $p_p = 0.4278$ bar. Since the permeability of the fractures is very high, the pressure along them is almost constant, therefore it does not make any appreciable difference to discretize them or not. The pressure fields obtained by the 2-D and 3-D strategies are at the same magnitude order, despite not being equivalent. These differences are expected since we did not use the same meshes. Even so, we consider that the strategy presented here is capable of satisfactorily including the influences of high permeability fractures in a 3-D domain adding just a few degrees of freedom to the original mesh (the rock matrix one) and without the necessity to build it (the rock matrix mesh) fitting the fractures positions, as we do when using the conforming mesh hybrid-grid method [14].

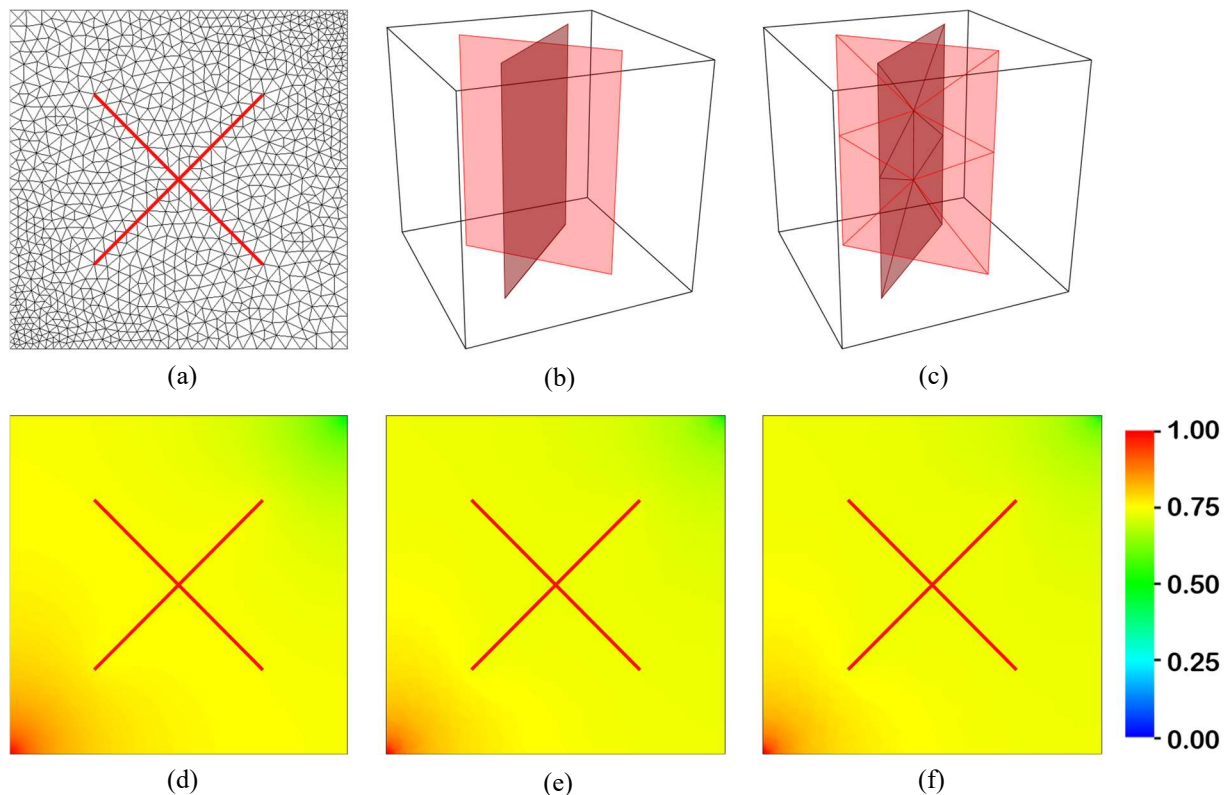


Figure 5 – Intersection between. (a) 2-D mesh. (b) Fractures in 3-D problem. (c) Discretization of the fractures in 3-D problem with 16 cells. (d) Solution of the 2-D through the strategy of Cavalcante et al. [14]. (e) Solution of the 3-D version of the same problem through here presented strategy using 2 fracture cells. (f) Solution of the 3-D version of the same problem through here presented strategy using 16 fracture cells.

5 Conclusions

In this work, we presented an embedded discrete fracture model (EDFM) to be applied on unstructured

tetrahedral meshes in context of one-phase flow in naturally fractured reservoirs. To discretize the elliptic pressure equation, we use the recently developed 3-D version of the multipoint flux approximation that uses the "diamond stencil" (MPFA-D). We have discretized the fractures by two ways, as 2 rectangular cells and as 16 triangular cells, without any noticeable differences, in terms of results between them. Since the permeability of the fractures is very high, the pressure along them is almost constant, therefore it does not make any appreciable difference to discretize them or not. When compared with the results obtained in 2-D by the conforming mesh hybrid-grid method presented by Cavalcante et al. [14], our strategy has also achieved good preliminary results, which are in the same magnitude order than those ones, but without the necessity to build the rock matrix mesh fitting the fractures positions, as we do when using the conforming mesh hybrid-grid method [14], and needing just adding a few degrees of freedom to the problem.

Acknowledgements. The authors thank the Foundation for Support of Science and Technology of Pernambuco (FACEPE), the National Council for Scientific Development (CNPq), the Coordination for Improvement of Higher Education Personnel (CAPES).

Authorship statement. The authors hereby confirm that they are the sole liable persons responsible for the authorship of this work, and that all material that has been herein included as part of the present paper is either the property and authorship of the authors.

References

- [1] Z.R. Beydoun, "Arabian plate oil and gas: Why so rich and so prolific?," *Episodes*. vol. 21, no. 2, pp. 74–81, 1998.
- [2] S.K. Matthäi, *Modelling multiphase flow in fractured porous rock*. , London, 2005.
- [3] D.K.E. de Carvalho, R.B. Willmersdorf, and P.R.M. Lyra, "Some results on the accuracy of an edge-based finite volume formulation for the solution of elliptic problems in non-homogeneous and non-isotropic media.," *International Journal for Numerical Methods in Fluids*. vol. 61, no. 3, pp. 237–254, 2009.
- [4] I. Aavatsmark, T. Barkve, O. Bøe, and T. Mannseth, "Discretization on Unstructured Grids for Inhomogeneous, Anisotropic Media. Part I: Derivation of the Methods.," *SIAM Journal on Scientific Computing*. vol. 19, no. 5, pp. 1700–1716, 1998.
- [5] V. Martin, J. Jaffré, and J.E. Roberts, "Modeling Fractures and Barriers as Interfaces for Flow in Porous Media.," *SIAM Journal on Scientific Computing*. vol. 26, no. 5, pp. 1667–1691, 2005.
- [6] H. Hoteit and A. Firoozabadi, "An efficient numerical model for incompressible two-phase flow in fractured media.," *Advances in Water Resources*. vol. 31, no. 6, pp. 891–905, 2008.
- [7] T. Manzocchi, J.J. Walsh, P. Nell, and G. Yielding, "Fault transmissibility multipliers for flow simulation models.," *Petroleum Geoscience*. vol. 5, no. 1, pp. 53–63, 1999.
- [8] G. Barenblatt, I. Zheltov, and I. Kochina, "Basic concepts in the theory of seepage of homogeneous liquids in fissured rocks [strata].," *Journal of Applied Mathematics and Mechanics*. vol. 24, no. 5, pp. 1286–1303, 1960.
- [9] L. Li and S.H. Lee, "Efficient Field-Scale Simulation of Black Oil in a Naturally Fractured Reservoir Through Discrete Fracture Networks and Homogenized Media.," *SPE Reservoir Evaluation & Engineering*. vol. 11, no. 04, pp. 750–758, 2008.
- [10] I. Berre, F. Doster, and E. Keilegavlen, "Flow in Fractured Porous Media: A Review of Conceptual Models and Discretization Approaches.," *Transport in Porous Media*. vol. 130, no. 1, pp. 215–236, 2019.
- [11] R.J.M. Lira Filho, S.R. Santos, T. de M. Cavalcante, F.R.L. Contreras, P.R.M. Lyra, and D.K.E. Carvalho, "A linearity-preserving finite volume scheme with a diamond stencil for the simulation of anisotropic and highly heterogeneous diffusion problems using tetrahedral meshes.," *Computers & Structures*. vol. 250, p. 106510, 2021.
- [12] M. Borsuk and V. Kondratiev, "The Dirichlet problem for elliptic linear divergent equations in a nonsmooth domain.," Presented at the (2006).
- [13] X. Rao, L. Cheng, R. Cao, P. Jia, H. Liu, and X. Du, "A modified projection-based embedded discrete fracture model (pEDFM) for practical and accurate numerical simulation of fractured reservoir.," *Journal of Petroleum Science and Engineering*. vol. 187, p. 106852, 2020.
- [14] T. de M. Cavalcante, F.R.L. Contreras, P.R.M. Lyra, and D.K.E. Carvalho, "A multipoint flux approximation with diamond stencil finite volume scheme for the two-dimensional simulation of fluid flows in naturally fractured reservoirs using a hybrid-grid method.," *International Journal for Numerical Methods in Fluids*. p. fld.4829, 2020.